Dynamic Soil Identification by means of Rayleigh Waves

V. Roma
Geodata S.P.a. Turin, Italy

ABSTRACT: In those engineering projects where external vibrations coming from different sources in the surroundings (i.e. seismic waves, railway, pile driving, industrial machines, highway, subway, explosions) are expected, the identification of dynamic characteristics of the soil (i.e. Damping and wave velocity profiles) is necessary to predict the soil-structure dynamic interaction. This work focuses on the dissipative properties of the soil, which are expressed in terms of attenuation or energy absorption coefficient, as it has been determined during Multichannel SASW (Spectral Analysis of Surface Waves) tests performed at several sites. From experimental results the variation of the attenuation coefficient with the frequency of excitation (attenuation curve), as predicted by the visco-elastic theory, has been confirmed. An attempt has been made to correlate soil nature and conditions to the possible limits of the attenuation coefficient in the frequency range of 5Hz÷100Hz.

1 INTRODUCTION

In many engineering projects the soil-structure interaction problem is solved where the external loads are represented by vibrations, which reach the structure travelling through the soil. In these cases the systems to be identified are the supestructure, the external source of vibrations and the ground which transmits the vibrations. Several works have been published about the characteristics of wave propagation and energy attenuation in the case of seismic events (Gazetas and Yegian 1979, Aki and Richards 1980). Nevertheless all these cases deal with a seismological spatial scale, that is different from the geotechnical scale. Other papers (Krylov et al. 2000, Kaynia et al. 2000) are concerned with the vibrations generated by high speed trains and how the induced waves propagate into the ground from the railway, but there is not much literature (Barkan 1962) about the correlation among attenuation coefficients (i.e. energy loss due to material damping) and soil characteristics. This work summarizes the results concerning the energy attenuation of Rayleigh waves as it has been determined during Multichannel SASW at different sites.

2 RAYLEIGH WAVES AND MULTICHANNEL SPECTRAL ANALYSIS OF SURFACE WAVES TEST

2.1 *Experimental set-up*

The Multichannel SASW test is a non-invasive technique (Roma 2001) that consists in measuring the wave field generated on the free surface by exciting the soil at a surface point (Fig.1). The point source can be either impulsive (i.e. hammer, falling weight) or harmonic (electromechanic shaker) and the receivers (geophones or accelerometers) are placed along a line departing from the source (Hebeler 2001). More recently environmental noise is used as excitation of the soil and the receivers are set up in concentric circles, since the source direction is not known a priori. In this case the method is called Passive Multichannel SASW, to be distinguished from the Active Multichannel SASW (Zywichy 1999). The main aspects to be considered in the experiments are the span between two consecutive receivers and the time interval of acquisition, so that aliasing problems can be avoided.

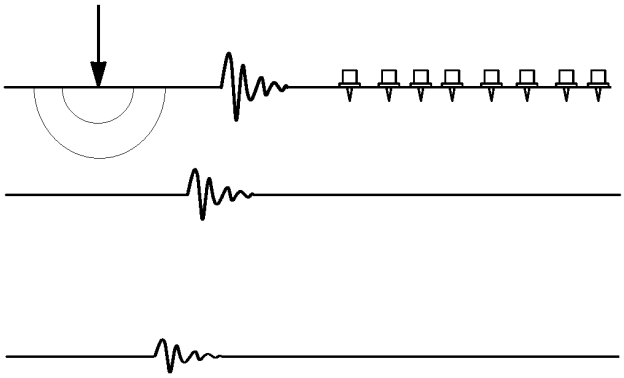

Figure 1. Scheme of the experiment in situ.

2.2 *Theoretical framework for evaluation of attenuation curves*

In the Multichannel SASW test the waves involved during the measurement of the wave field on the free surface of the ground are primarily Rayleigh waves. Rayleigh waves are responsible for energy transmission at long distances from the source, as it has been recognized during seismic events (Ewing et al. 1957). The use of dispersive properties of Rayleigh waves in a multilayered system to identify the shear wave velocity profile and the Q factor is not new for seismologists (Nolet and Panza 1976, Vuan et al. 1995, Jongmans et al. 1993). During propagation of Rayleigh waves two distinct phenomena can be discerned: 1) wave dispersion and 2) wave amplitude attenuation.

The wave dispersion phenomenon occurs when the several harmonic components of a whole disturbance separate during propagation, because of their different energy or group speeds (Lighthill 1964). As a consequence of dispersion the apparent phase velocity of Rayleigh waves varies with the frequency of excitation. For the particular case of a homogeneous half-space dispersion does not happen and the apparent phase velocity is constant with frequency and it is equal to the apparent group velocity. On the basis of the dispersion phenomenon the shear wave velocity profile can be inferred by means of the so called uncoupled inversion procedure (Roma 2002). The attenuation phenomenon concerns both the geometrical attenuation of wave amplitude, due to the shape of the spreading wave-fronts, and the material attenuation of the wave field, caused by energy losses associated to interparticle friction. The material attenuation is strictly linked to the damping ratio profile and also coupling exists between dispersion and attenuation phenomena accordingly to the principle of causality, as it is stated by the Kramers-Kroning relation (Aki and Richards 1980, Lai 1998). Nevertheless at very small deformation level ($\gamma_{cyclic} \leq 5 \cdot 10^{-6} \div 5 \cdot 10^{-5}$ Vucetic 1994), the coupling effects between attenuation and dispersion (i.e. between wave velocity and damping ratio) can be neglected and results from uncoupled method and coupled method are comparable (Roma 2003). In the following, reference will be done only to the uncoupled method.

From the wave field measurements the experimental displacement transfer function (system response to harmonic excitation) $T_{exp}(r,\omega)$ of the site is calculated. If the particle accelerations are measured, then the experimental displacement transfer function of the system is (Lai et al. 2002):

$$T_{\exp}(r,\omega) = \frac{-M(r,\omega)\cdot C_2(\omega)}{\omega^2 \cdot C_1(\omega)} \tag{1}$$

where ω is the circular frequency of excitation, r is the distance from the source, $M(r,\omega)$ is the ratio of the particle acceleration measured at the receiver to the input force measured at the

source. $C_1(\omega)$ and $C_2(\omega)$ are the frequency-dependent calibration factors of the accelerometers used to detect the particle motion and the accelerometer placed on the shaker, respectively. The factor $C_2(\omega)$ also includes the mass of the armature of the shaker.
The theoretical expression of the displacement transfer function $T_{theo}(r,\omega)$ of the system is:

$$T_{theo}(r,\omega) = \frac{U_z(r,\omega,t)}{F_z \cdot e^{i\omega t}} = G(r,\omega) \cdot e^{-i\cdot\Psi(r,\omega)} \tag{2}$$

where F_z is the magnitude of the exciting force, $U_z(r,\omega,t)$ is the vertical displacement, $G(r,\omega)$ is the geometric spreading function of Rayleigh waves, $\psi(r,\omega)$ is the apparent phase of the wave train, which contains all Rayleigh waves. It should be noted that near field effects due to P and S waves are not considered and only Rayleigh waves are taken into account in the theoretical formulation. Also the contribution of higher modes of Rayleigh is ignored in the apparent phase $\psi(r,\omega)$, so that only the fundamental mode appears in the phase $\psi(r,\omega)\cong k^*_R(\omega)\cdot r$ and (2) becomes:

$$T_{theo}(r,\omega) \cong G(r,\omega) \cdot e^{-i\cdot K^*_R(\omega)\cdot r} \tag{3}$$

To estimate the complex apparent wavenumber:

$$K^*_R(\omega) = \left[\frac{\omega}{V_R(\omega)} - i\alpha_R(\omega)\right] \tag{4}$$

that appears in equation (3), the distance between the experimental end the theoretical system response has to be minimized at each frequency ω:

$$\sum_{i=1}^{i=N} \left| T_{exp}(r_i,\omega) - T_{theo}(r_i,\omega) \right| = dis\tan ce(\omega) \tag{5}$$

where the subindex i refers to the i-th receiver.
In the coupled method both the apparent phase velocity $V_R(\omega)$ and the apparent attenuation coefficient $\alpha_R(\omega)$ in equation (4) are searched at each frequency ω, whereas in the uncoupled method the shear wave velocity profile is evaluated in the first step of the inversion procedure. Hence in the second step the apparent phase velocity $V_R(\omega)$ is known and only the apparent attenuation coefficient $\alpha_R(\omega)$ remains to be determined. The optimisation problem stated by equation (5) has been solved by means of the Levenberg Marquardt non-linear inversion algorithm (Press et al. 1992, Rix et al. 1999).
In Figure 2 the comparison between the experimental (circles) and the theoretical (dots) absolute value of the vertical displacements is illustrated at the frequencies between 15Hz and 21.25Hz for the investigated site Mud A (see section 3).
In the diagram of Figure 2 the oscillating behaviour of both the responses due to the superposition of all the Rayleigh modes can be noted. This aspect assumes relevance when dealing with inversely dispersive sites, especially at frequencies greater than the cut-off frequency of the second mode of Rayleigh. In fact below the cut-off frequency of the second mode of Rayleigh only the fundamental mode exists and the Geometrical Spreading Rayleigh function $G(r,\omega)$ reduces to a constant factor proportional to $1/\sqrt{r}$ that governs the geometrical attenuation law of the Rayleigh waves through a homogeneous half-space (Roma et al. 2002). From the attenuation coefficients $\alpha_R(\omega)$ determined at each frequency ω the attenuation curve can be obtained, in which the variation of the attenuation with frequency is plotted (see Fig. 10).

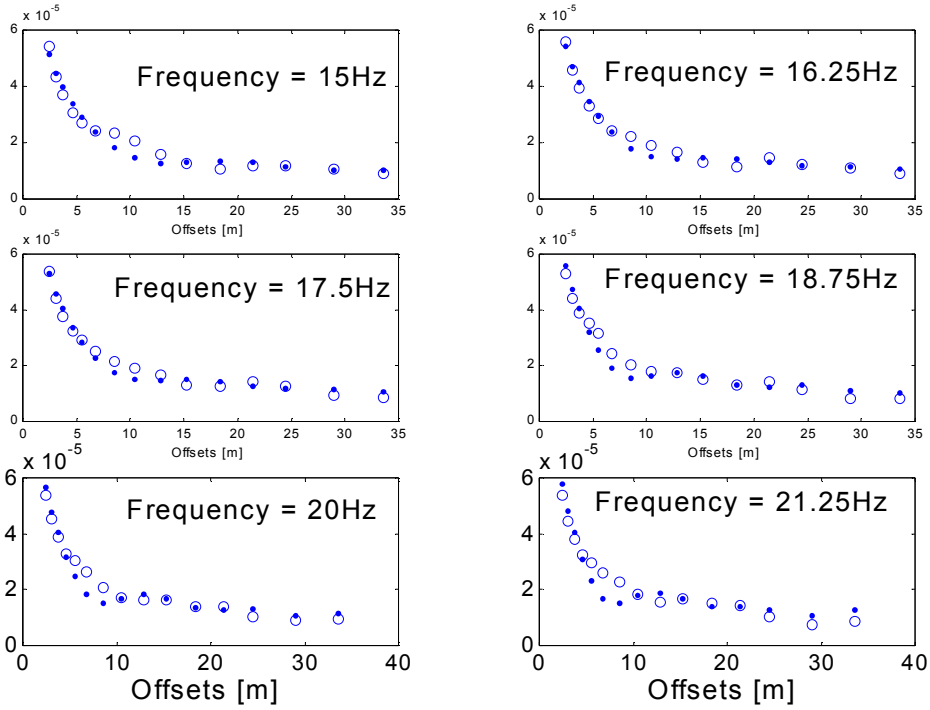

Figure 2: Experimental (circles) and the theoretical (dots) absolute value of the vertical displacements at site Mud A.

3 INVESTIGATED SITES

3.1 *Description of the sites*

The above illustrated method has been applied to several sites while performing the Multichannel SASW test for determining the shear wave velocity profile and the damping ratio profile. The results refer to very small strain level, since the maximum shear strain measured during SASW test is nearly $\gamma=(1\div5)\cdot10^{-5}$ (Roma 2003).

3.1.1 *Site S16*

This site is located in Germantown near Memphis, Tennessee (U.S.) at approximately 100m to the south of Nonconnah Creek river and is part of the Memphis-Shelby County Hazard Mapping Project as the other sites in the Memphis area which are reported in Table 8. Unfortunately the stratigraphic profile is not available for this site. Nevertheless the site is within the floodplain of Nonconnah Creek and it can be inferred that the surface soils are of young geologic age. The only sure information is the existence of a surficial layer of very cracked clay, recognized during the experiment (Hebeler 2001). Also the water table position has been estimated at a depth of approximately 3.5m. On this site the Multichannel SASW method has been applied to identify the shear wave velocity Vs and the shear damping ratio Ds profiles (see Table 1, Fig.3).
The site is normally dispersive and belongs to the class B, according to the Eurocode 8.

Table 1, Figure 3 : Shear wave velocity Vs and shear damping ratio Ds profiles at site S16.

h (m)	Vs (m/s)	Ds (%)
3.5	190	5.0
3	245	5.1
5	280	5.1
3.5	280	5.1
5.5	375	5.1
9.5	480	5.1
7.7	595	5.1
Half-space	795	5.1

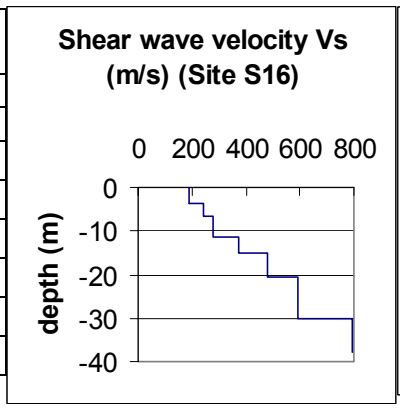

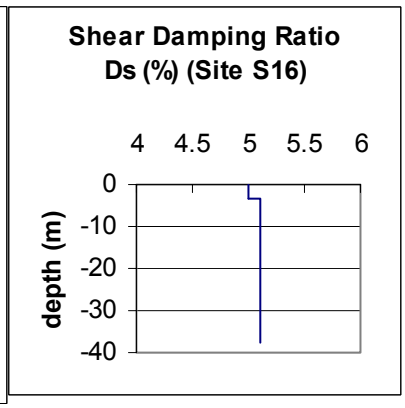

3.1.2 *Site Houston Levee Park*

The site is located in the alluvial deposits of Wolf river in Germantown near Memphis, Tennessee (U.S.). The ground consists of alternating layers of clayey silt and sands down to a depth of about 10m, where the stiff clay of Jackson Formation is encountered, which reaches a depth greater than 20m. The water table depth is 5m (Schneider and Mayne 1999). In Table 2 and Figure 4the shear wave velocity Vs and the shear damping ratio Ds profiles inverted by means of Multichannel SASW method are presented.

Table 2, Figure 4: Shear wave velocity Vs and shear damping ratio Ds profiles at site Hous ton Levee Park.

h (m)	Vs (m/s)	Ds (%)
2	155	4.6
2	200	5.7
2	240	6.0
2	285	6.1
3	295	6.1
3	315	6.1
3	325	6.1
Half-space	355	6.1

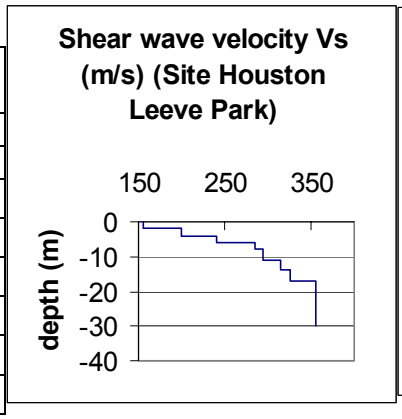

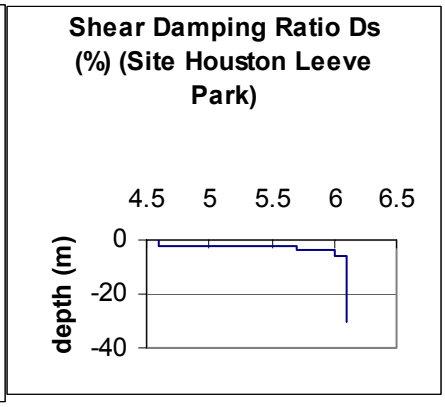

As in the case of the site S16, the site Houston Levee Park belongs to the class B of the Eurocode 8. The site is normal dispersive with a regular profile, since stiffness monotonically increases with depth.

3.1.3 *Sites Mud A and B*

These two sites are located in different places of the man-made Mud Island in Downtown Memphis, Tennessee (U.S.). The Mud Island was formed prevalently by hydraulic filling and partly by natural sedimentation from the Mississippi River. The profile of both sites is constituted by alternating layers of silt and loose sand down to a depth of at least 25m, where a more dense layer of sand exists. The water table is at a depth of 8m. As for the other sites the SASW

test has been performed and the resulting shear wave velocity Vs and the shear damping ratio Ds profiles are summarized in Tables 3,4 and Figures 5,6 below.

Table 3,Figure 5:Shear wave velocity Vs and shear damping ratio Ds profiles at site Mud A.

h (m)	Vs (m/s)	Ds (%)
1	145	1.2
1	155	1.4
1	160	1.1
0.8	165	0.7
1	175	0.4
1	145	0.2
1	160	0.1
2	165	0.07
3.2	160	0.05
2	175	0.05
3	180	0.05
3	200	0.05
4	225	0.05
4	250	0.05
Half-space	390	0.05

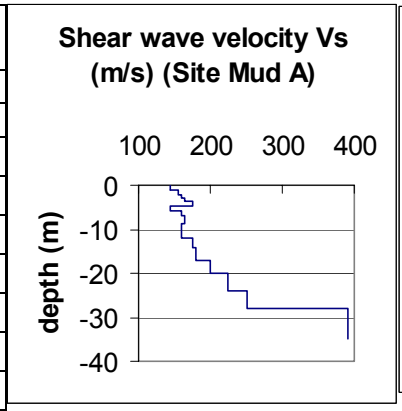

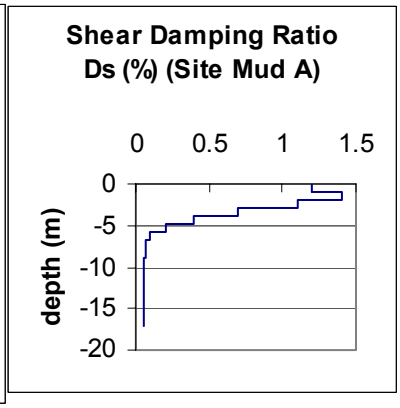

This site shows an essentially normally dispersive profile, with very low values of shear damping ratio Ds, compared to the other sites.

Table 4,Figure 6: Shear wave velocity Vs and shear damping ratio Ds profiles at site Mud B.

h (m)	Vs (m/s)	Ds (%)
1.5	195	1.5
1.5	180	1.3
2.5	170	1.4
2.5	170	1.8
5	165	3.3
6	190	3.5
7	280	3.5
10	225	3.5
Half-space	665	3.5

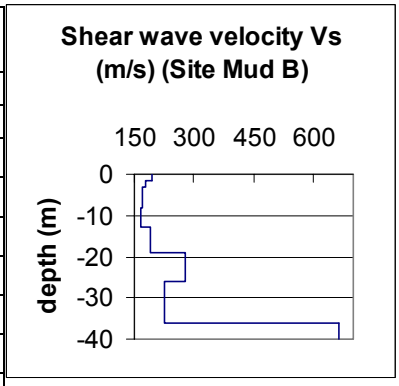

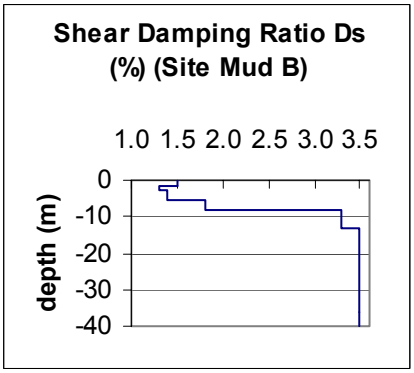

The profile is slightly inversely dispersive, because there are some soft layers trapped between stiff layers. The shear damping ratio Ds is low.

3.1.4 *Site Pisa Tower*

This site is definitely the most investigated of all, because of the importance of the Leaning Tower of Pisa. The MSASW test has been performed near the Lupa monument. In Table 5 the

stratigraphy of the site is briefly described (Lo Presti et al. 2002). The upper part of the site (from 3 m a.s.l. down to 0 m a.s.l.) is formed by a heterogeneous silty-clayey soil containing archaelogical remains. Below this man-made stratum there is the horizon A, consisting of strata of silt and sand of various thickness (from 0 m a.s.l. to -7.5 m a.s.l.). From -7.5 m a.s.l. to- 40 m a.s.l. there are the clays of the horizon B and below -40m a.s.l. there is the horizon C made of sands. The phreatic water level within the horizon A varies between 1m and 1.5m below the free surface.

Table 5, Figure 7: geotechnical profile with wave velocity Vs and shear damping ratio Ds profiles at site Pisa Tower.

h (m)	Vs (m/s)	Ds (%)	layer	Thickness (m)	description
1.5	190	4.35	Man-made	3	Silt and clay
1.5	170	3.9	Horizon A	7.5	Silt and sand
3	175	3.25	Horizon B	32.5	Clay and sand
2.5	150	2.3	Horizon C	20	sand
3	140	2.35			
5	200	2.3			
5	250	2.3			
Half-space	300	2.3			

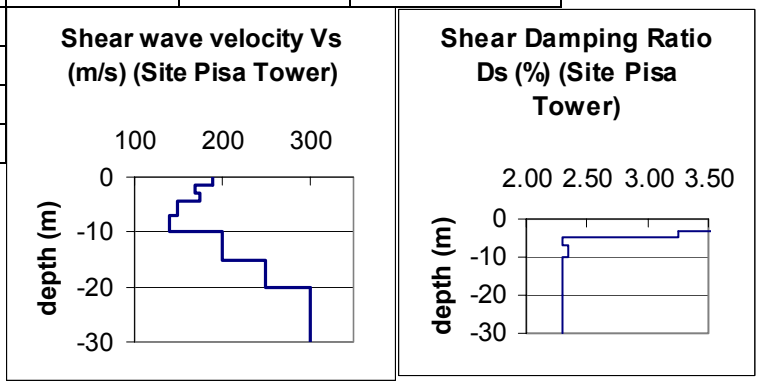

3.1.5 *Site Jackson County Landfill*

The site is located in the Jackson County Landfill near Amagon in Arkansas (U.S.). At the moment of the SASW test the ground consisted of a cracked surficial layer of clay, which overlays a medium to dense thick layer of sand. There is no information about the ground water table.

Table 6, Figure 8: Shear wave velocity Vs and shear damping ratio Ds profiles at site Jackson County Landfill.

h (m)	Vs (m/s)	Ds (%)
2	125	3.75
2	165	1.1
2	210	0.9
2	220	0.8
3	220	0.8
3	215	0.8
3	215	0.8
4	220	0.8
4	235	0.8
4	255	0.8
5	270	0.8
Half-space	285	0.8

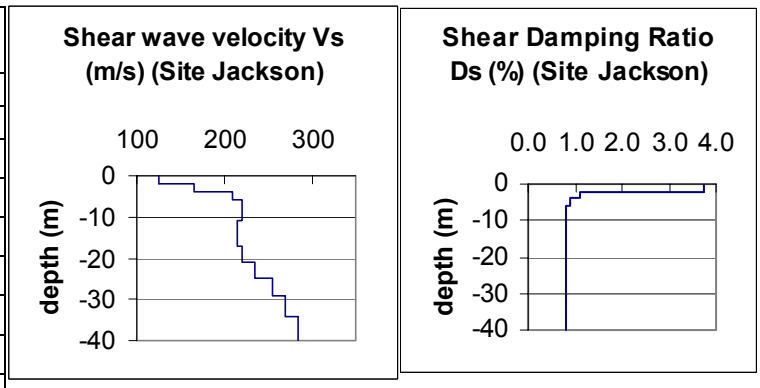

3.1.6 *Site Treasure Island*

This site is located in the San Francisco Bay and is on an artificial island made of hydraulic filling. The profile consists of a surficial layer of gravelly sand over 10m of loose, fine-to-medium sand, underlain by 12m-18m of soft clay. The water table is approximately at the depth of 1.5m. The SASW test has been conducted by Lai and Rix (Rix, Lai, Spang 1999) and the results give information down to a depth of 15m. The shear wave velocity profile below the depth of 15m has been taken from other references (Lanzo G.and Silvestri F. 1999). The stratigraphy is presented in Table 7 and Figure 9.

Table 7, Figure 9: Shear wave velocity Vs and shear damping ratio Ds profiles at site Treasure Island.

h (m)	Vs (m/s)	Ds (%)
1.8	145	0.6
1.7	130	2
1.5	135	1.8
2.5	145	1
3.5	155	0.5
17	165	0.25
15	265	0.25
60	250	0.25
Half-space	1000	0.25

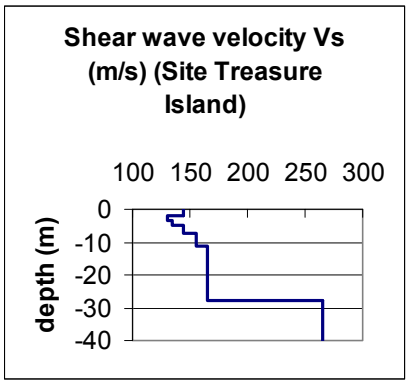

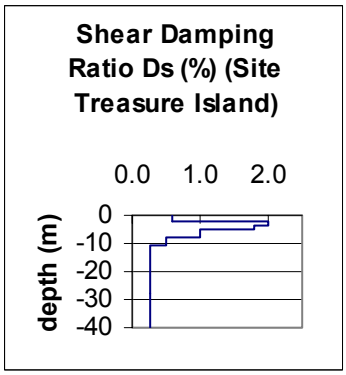

Table 8: sites which have been analysed.

Site	Location	description	Water table depth (m)	Vs_{30} (m/s)	Ds_{30} (%)	Ds_1 (%)	Class
S16	Memphis, Tennessee (U.S.)	Cracked superficial layer of clay	3.5	314	5.1	5.0	B
Houston Levee Park	Memphis, Tennessee (U.S.)	Superficial layer of clayey silt over layer of sand over a halfspace of stiff clay	5	289	5.9	4.6	B
Mud A	Memphis, Tennessee (U.S.)	Loose sedimentary layers of silt and sand	5	198	0.1	1.2	C
Mud B	Memphis, Tennessee (U.S.)	Loose sedimentary layers of silt and sand	8	200	2.6	1.5	C
Pisa Tower	Pisa (Italy)	layers of man-made ground, silt, sand and clay	3	206	2.5	4.35	B
Jackson County Landfill	Amagon, Arkansas (U.S.)	Very stiff superficial layer of clay over medium to dense sand	Not available	210	0.9	3.75	B
Treasure Island	San Francisco, California (U.S.)	Loose fine-to-medium sand on soft clay (bay mud)	1.5	160	0.3	0.6	C

In Table 8 the list of the investigated sites is reported, with a summary of the site description, the water table position, the averaged shear wave velocity Vs_{30} and shear damping ratio Ds_{30} within the depth of 30m from the free surface:

$$Vs_{30}=\Sigma(h_i)/\ \Sigma(h_i/Vs_i), \qquad Ds_{30}=\Sigma(h_i)/\ \Sigma(h_i/Ds_i) \tag{6, 7}$$

where h_i is the thickness of the i-th layer and Ds_{30} has been defined as done for Vs_{30}. Also the class of the soil has been evidenced according to EC 8 classification for local site effects
The results obtained at the above specified sites compare well with other investigations, which specify a range for shear damping ratio Ds at very small deformations for different soils (see Table 9).

Table 9: range of shear damping ratio Ds (in %) for different soils at very small deformations (Bowles 1996)

Soil type	**Stewart & Campanella (1993)**	**Others**
Clay	1.0÷5	1.7÷7
Silt	-	2.5
Alluvium	-	3.5÷12
Sand	0.5÷2	1.7÷6

It can be observed that energy dissipation of travelling waves is generally low for silt and increases for sand, clay and alluvial soils.

Following the method explained in section 2, the variation of the energy absorption coefficient $\alpha_R(f)$ as a function of frequency f has been plotted in Figure 10 for all the above analysed sites.

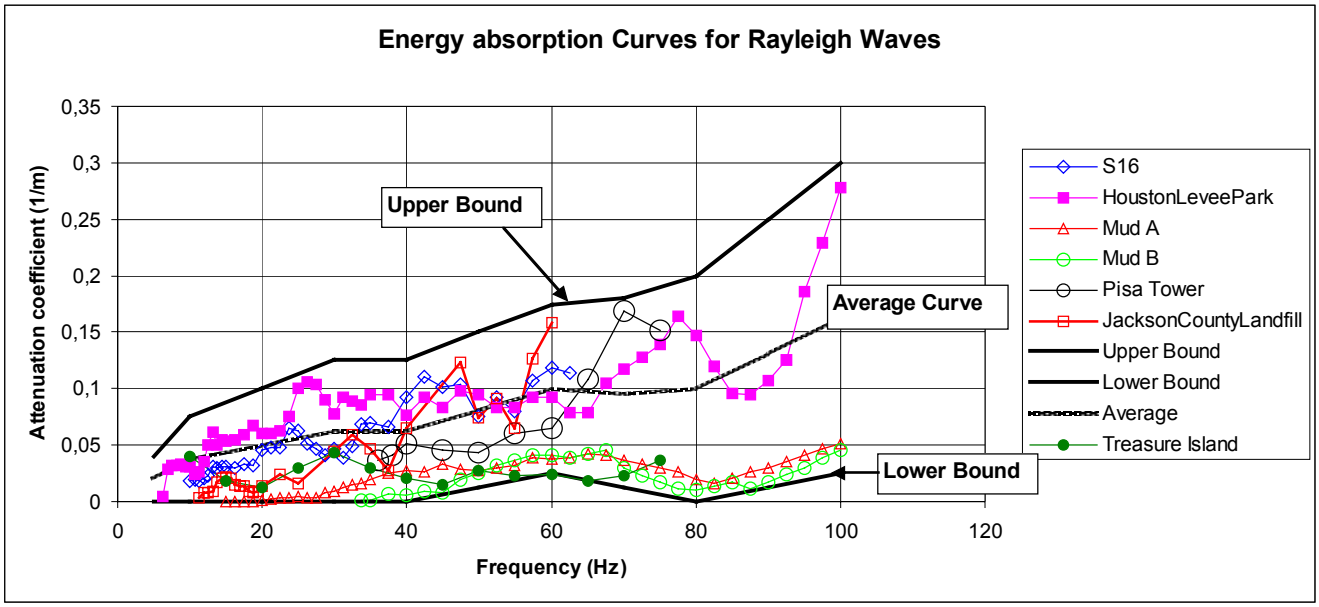

Figure 10. Attenuation coefficient α of Rayleigh waves for different sites.

The attenuation coefficient α is strictly correlated to damping ratio Ds (Rix et al. 1999), so it is expected that to high values of Ds correspond high values of attenuation coefficient α. Shear damping ratio Ds depends on the site characteristics such as soil nature, strain level γ, overconsolidation ratio OCR, degree of saturation, confining pressure, plasticity index IP for cohesive soils, void ratio e, friction angle ϕ' for non cohesive soils. For sands and gravelly soils it has been found (Seed et al. 1986) that shear damping ratio Ds increases if void ratio e , friction angle ϕ', degree of saturation, OCR and confining pressure decrease. For clays other researchers

(Vinale et al. 1996) have observed that Ds increases if plasticity index IP increases and if OCR decreases.
Unfortunately only few of the presented sites have been adequately investigated by means of laboratory and in situ tests, so at this stage of knowledge the available information is not sufficient to clarify the link of the attenuation curves with factors such as overconsolidation ratio OCR, degree of saturation, plasticity index IP, void ratio e, friction angle ϕ' and confining pressure.
Nevertheless the following conclusions can be inferred. As a general trend common to all the sites the attenuation of surface waves increases as the frequency of the vibration increases. This result was expected, since at higher frequencies the number of oscillations of the particles around their equilibrium configuration increases. If it is considered that during transmission the mechanical wave loses energy at each cycle, the total amount of dissipated energy depends on the number of cycles per unit of time, that is the frequency of the wave. The range of frequencies that has been considered is between 5Hz and 100Hz. In Figure 10 two curves have been introduced, which delimit the upper and the lower bounds of all the attenuation curves at the several sites and a third curve has been plotted, which is the average of the upper bound and the lower bound curves. The average curve is representative of the trend of the average attenuation coefficient $\alpha_{average}$, which within the above specified frequency range varies essentially linearly from α_{min}=0.025·1/m at f=5Hz to α_{max}=0.15·1/m at f=100Hz.. From Figure 10 two distinct trends can be distinguished inside the belt delimited by the upper and lower bounds curves. The first trend is characterized by attenuation curves near the lower bound curve with low values of the attenuation coefficient α. This behaviour is common to the three sites Mud A, Mud B and Treasure Island. All the other analysed sites belong to the second trend, characterized by higher values of the attenuation coefficient α. The first distinction among the three sites Mud A, Mud B and Treasure Island and the other sites is that the former group of sites is represented by artificial islands, which have been recently formed by hydraulic filling of silt and sand. On the contrary the remaining sites are naturally formed soils. The different dynamic behaviour between the two groups of sites can be also explained in terms of shear damping ratio Ds_1 of the superficial layer, rather than of the averaged shear damping ratio Ds_{30} within the first 30m of ground. In fact the sites Mud A, Mud B and Treasure Island shows shear damping ratio Ds_1 less than 2.0% on the free surface, where surface waves and Rayleigh waves mainly propagate.
The values of α reported in Figure 10 are in good agreement with results obtained by Barkan (Barkan 1962), who made an extensive campaign of experimental measurements of vibrations produced by real machines. His investigations cover several types of soils in different conditions at frequencies ranging between 10Hz and 30Hz (see Table 10). From Barkan's results it can been inferred that energy absorption is lower in frozen and organic soils.

Table 10: attenuation coefficient α for several soil types and conditions at frequencies in the range 10Hz÷30Hz

Soil description	**α (1/m)**
Yellow water-saturated fine-grained sand	0.100
Yellow water-saturated fine-grained sand in a frozen state	0.060
Gray water-saturated sand with laminae of peat and organic silt	0.040
Clayey sands with laminae of more clayey sands and of clays with some sand and silt, above ground-water level	0.040
Heavy water-saturated brown clays with some sand and silt	0.040÷0.120
Marly chalk	0.100
Loess and loessial soils	0.100

3.2 *Utility of the attenuation coefficient α*

In order to better comprehend the usefulness of the attenuation coefficient α for engineering purposes, consider the problem of determining the amplitude of vibrations generated by any

source (i.e. railway, traffic, industrial machine, subway, workings, explosions) on buildings and structures foundations placed at a distance x from the source.
In a simplified analysis the contribution of higher modes of propagation can be omitted and only the fundamental mode is considered. This is true for homogeneous sites or for normally dispersive sites, where ground stiffness increases with depth. Under this assumption the vibration amplitude on the free surface A(x) at a distance x (for example x=10m) from the source on the free surface can be expressed as:

$$A(x)=A(x_0)\cdot(x_0/x)^{0.5}\cdot e^{-\alpha(x-x_0)} \quad (8)$$

where $A(x_0)$ is the known amplitude at the distance x_0 from the source (for example $A(x_0)$=10mm at x_0=0.1m).
If the dominant frequency f_{mean} (say f_{mean}=50Hz for an industrial machine) of the exciting source is known and no specific tests on the ground dynamic properties have been performed at the site, then the corresponding value of the attenuation coefficient α_{mean} can be evaluated from the average curve of the Figure 10 (at f_{mean}=50Hz α_{mean}=0.075·1/m) and the amplitude at a distance x=10m can be approximately estimated equal to 0.5mm. If the dominant frequency of the exciting source is f_{mean}=5Hz (i.e. train, tram), then α_{mean}=0.025·1/m and for the same $A(x_0)$=10mm at x_0=0.1m, the vibration amplitude at a distance x=10m is equal to 0.8mm.
If the frequency spectrum of the source is available, then the frequency response of the ground at the distance x can be calculated by applying equation (8) to each frequency component.

4 CONCLUSIONS

The variation of the attenuation coefficient α within the frequency range 5Hz÷100Hz (attenuation curve) has been determined for several sites, for which shear wave velocity Vs and shear damping ratio Ds profiles have been reported, together with available information on stratigraphy. By considering the attenuation curves of all the analysed sites an upper and a lower bound curves have been determined. From the upper and lower bounds an average curve has been determined, which is a pragmatic tool to do approximate, but immediate predictions of the degree of vibration transmission through the surface of the soil. Also an attempt has been made to associate the frequency dependent value of the attenuation coefficient α to the soil nature and conditions. Unfortunately only few of the presented sites have been adequately investigated by means of laboratory and in situ tests, so additional efforts are needed to gain more knowledge about the link of the attenuation curves with factors such as strain level, overconsolidation ratio OCR, degree of saturation, plasticity index IP, void ratio e, friction angle ϕ' and confining pressure.

BIBLIOGRAPHY

Achenbach, J.D. 1999. Wave Propagation in Elastic Solids. North-Holland, Amsterdam, Netherlands.

Aki K. and Richards P.G. 1980. Quantitative Seismology, Theory and Methods, Vol. 1-2 W.H. Freeman & Co., N. York.

Barkan D.D. 1962. Dynamics of bases and foundations. McGraw-Hill

Bowles J.E. 1996. Foundation Analysis and Design. Fifth edition, McGraw-Hill, N.Y.

Christensen, R.M. 1971. Theory of viscoelasticity - an introduction", Ed. Academic Press

Ewing, W.M., Jardetzky, W.S., and Press, F. 1957. Elastic Waves in Layered Media. McGraw-Hill, New York, NY.

Gazetas G., Yegian M.K. 1979. Shear and Rayleigh Waves in Soil Dynamics. Journal of the Geotechnical Engineering Division. ASCE, Vol. 105, No. GT12

Hebeler G.L. 2001. Site characterization in Shelby County, Tennessee using advanced surface wave methods. Master's thesis. Georgia Institute of Technology.

Jongmans, D. and Demanet, D. 1993. The Importance of Surface Waves in Vibration Study and the use of Rayleigh Waves for Estimating the Dynamic Characteristics of Soils. Engineering Geology, Vol. 34, pp. 105-113.

Kaynia A.M., Madshus C., Zachrisson P. 2000. Ground vibration from high-speed trains: prediction and countermeasures. Journal of Geotechnical and Geoenvironmental Engineering, Vol. 126, No 6, pp.531-537

Krylov V.V., Dawson A.R., Heelis M.E and Collop A. C. 2000. Rail movement and ground waves caused by high-speed trains approaching track-soil critical velocities. Proceedings Institutions of Mechanical Engineers, Vol.214, pp.107-116.

Lai C.G. 1998. Simultaneous inversion of Rayleigh phase velocity and attenuation for near-surface site characterization, PhD Diss., Georgia Inst. of Techn., Atlanta (Georgia, USA)

Lai G., Rix G., Foti S., Roma V. 2002. Simultaneous Measurement and Inversion of Surface Wave Dispersion and Attenuation Curves, Journal of SDEE 22

Lanzo G., Silvestri F. 1999. Risposta Sismica Locale. Hevelius Edizioni

Lighthill, M.J. 1964. Group Velocity, J. Inst. Maths Applics, 1, 1-28

Lo Presti D., Jamiolkowski M., Pepe M. 2002. Geotechnical characterisation of the subsoil of the Pisa Tower. International Workshop on Characterisation and Engineering Properties of Natural Soils, Singapore, November

Nolet G. and Panza G.F. 1976 . Array analysis of seismic surface waves: limits and possibilities. Pure and applied Geophysics, 114.

Press W.H., Teukolsky S.A., Vetterling W.T., Flannery B.P. 1992. Numerical Recipies in Fortran- The Art of Scientific Computing. Cambridge (UK), Cambridge University Press, 2nd Edition

Rix G.J., Lai C.G., Wesley Spang A.W. Jr 1999. In situ measurement of damping ratio using surface waves, J. Geotech.and geoenvir. Eng., ASCE

Rix G, Hebeler G., Lai G., Orozco C., Roma V. 2001. Recent Advances in surface Wave Methods for Geotechnical Site Characterization, XV International Conference on Soil Mechanics and Geotechnical Engineering, Istanbul 27-31 August

Roma V. 2001. Soil Properties and Site Characterization by means of Rayleigh Waves. Ph.D Dissertation, Politecnico di Torino (Italy)

Roma V., Lancellotta R., Rix G.J. 2001. Rayleigh Waves in Horizontally Stratified Media: Relevance of Resonant Frequencies, WASCOM 2001 (Wave Stability in Continuous Media), Porto Ercole, June

Roma V. 2002. Automated Inversion of Rayleigh Geometrical Dispersion Relation for Geotechnical Soil Identification, 3rd WCSC (World Conference on Structural Control), Como

Roma V., Hebeler G., Rix G.J., Lai C.G. 2002. Geotechnical Soil Characterisation using Fundamental and Higher Rayleigh Modes Propagation in Layered Media, 12th ECEE (European Conference Earthquake Engineering), London, September

Roma V. 2003. Soil Properties and Site Characterization through Rayleigh Waves. Deformation Characteristics of Geomaterials, IS Lyon, September

Seed H.G. et al.1986. Moduli and Damping factors for Dynamic Analysis of Cohesionless Soils. JGED, ASCE, vol. 112, GT 11 pp1016-1032

Schneider J.A. and Mayne W.P. 1999. Soil Liquefaction Response in Mid-America Evaluated by Seismic Piezocone Tests. Mid-America Earthquake Report MAE-GT-3A, October 1999

Spang, A.W. 1995. In Situ Measurements of Damping Ratio Using Surface Waves, Master's Thesis, Georgia Institute of Technology, Atlanta, GA

Stewart W.P and Campanella R.G. 1993. Practical Aspects of in Situ Measurements of Material Damping with the SCPT. CGJ Vol.30, No 2 pp211-219

Stokoe II & Santamarina 2000. Seismic-Wave-Based Testing in Geotechnical Engineering , Melbourne

Thomson, W.T. 1950. Transmission of Elastic Waves Through a Stratified Solid, Journal of Applied Physics, Vol. 21, pp. 89-93.

Tolstoy 1973. Wave propagation, McGraw-Hill, New York

Vinale F., Mancuso C., Silvestri F. 1996. Dinamica dei terreni. Manuale di Ingegneria Civile, Vol. 1 Ed. Scientifiche A. Cremonesi

Vuan A., Costa G. Suhadolc P., Panza G.F. 1995. In situ measurements of dynamic parameters of soils. Field Measurements in Geomechanics, 4th International Symposium, Bergamo, Italy

Vucetic M. 1994. Cyclic threshold shear strains in soils, J. Geotechnical Eng. , vol. 120 (12) , ASCE, pp. 2208-2228

Zywicki D. and Rix G.J. 1999. Frequency-wavenumber analysis of passive surface waves. Proc. Symp. on the Appl. of Geophysics to Environm. and Eng. Problems, Oakland, pp. 75-84

Zywicki, D.J. 1999. Advanced Signal Processing Methods Applied to Engineering Analysis of Seismic Surface Waves. Ph.D. Dissertation, Georgia Institute of Technology